

# Experiment and CFD simulation of exhaust tube in high-voltage circuit breaker

Xiangyang Ye<sup>a</sup>, Francesco Pisu, Stephan Grob, Mahesh Dhotre and Javier Mantilla

*Interruption Development, ABB Ltd., 5401 Baden, Switzerland*

**Abstract.** In a high-voltage circuit breaker, the exhaust tube connects the arc zone with the exhaust volume. During the arc interruption process, the exhaust tube transports the hot gas from the arc interruption zone to the exhaust volume through its distributed holes. The design of a high performance exhaust tube in the circuit breaker development aims for well controlled hot gas evacuation mass flow and pressure waves. In this paper, the exhaust tube behaviour is investigated using Computational Fluid Dynamics (CFD). To verify the CFD simulation, a basic experimental study with pressure measurements at different positions of the exhaust tube is performed. Further, the design parameters influencing the exhaust tube behaviour and circuit breaker performance are investigated and discussed.

## 1 Introduction

In an electrical transmission network, high-voltage circuit breakers interrupt short circuit currents in order to protect the network and apparatus. Switching gas with good dielectric and thermodynamic properties such as SF<sub>6</sub>, or recently, a mixture of C<sub>5</sub>F<sub>10</sub>O/CO<sub>2</sub>/O<sub>2</sub> [8] with low Global Warming Potential (GWP), are used to extinguish the electric arc, which occurs after separation of the electrical contacts.

In a high-voltage circuit breaker, the exhaust tube is a tube connecting the arc zone with the exhaust volume as shown in Figure 1. During the arc interruption process, an electric arc occurs between the arcing contacts (tulip finger and plug). Polytetrafluoroethylene (PTFE) vapour, resulting from the nozzle ablation, is driven by the high pressures between the arcing contacts as an energy carrier with high temperature into the heating volume, so that a pressure is built up in the heating volume. When the current approaches zero, the arc pressure between the contacts collapses, allowing the gas to flow back from the heating volume into the opening gap between arcing contacts at high velocity to extinguish the arc. The exhaust tube transports the hot gas from the arc interruption zone to the exhaust volume through its distributed holes. As, The hot gas mass flow, pressure distribution, and pressure waves traveling along the length of the exhaust tube at the downstream region of the arcing zone play a big role for the upstream arc zone region and on the cooling of the arc in the current interruption. Further, it influences the metal erosion behaviour of the upstream arcing contacts. Therefore, the design of a high performance exhaust tube aims for a well-controlled hot gas evacuation mass flow and pressure wave.

---

<sup>a</sup> Corresponding author : [xiangyang.ye@ch.abb.com](mailto:xiangyang.ye@ch.abb.com)

In this paper, the effects of different geometry parameters, e.g., position and area of the exhaust tube holes, on the exhaust tube performance are investigated using Computational Fluid Dynamics (CFD). To verify the CFD simulation, basic experimental study with pressure measurement at different position of exhaust tube is performed, and the result compared with the simulation. Based on the CFD simulation and the experimental study, the behaviour of an exhaust tube and its effects on the circuit breaker performance is investigated. Further, the design parameters influencing the exhaust tube behaviour and circuit breaker performance are investigated and discussed.

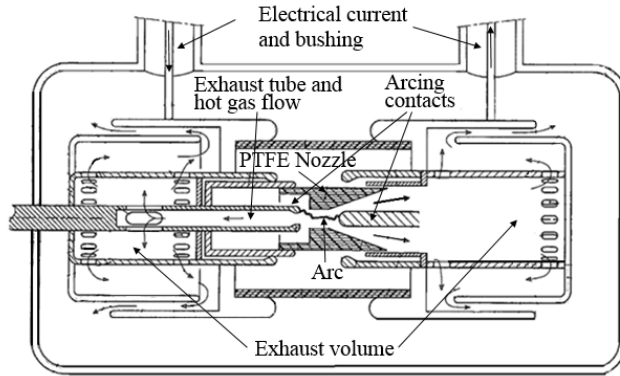


**Figure 1.** High-voltage circuit breaker and exhaust tube.

## 2 Experimental set-up

### 2.1 Experimental set-up for the exhaust tube study

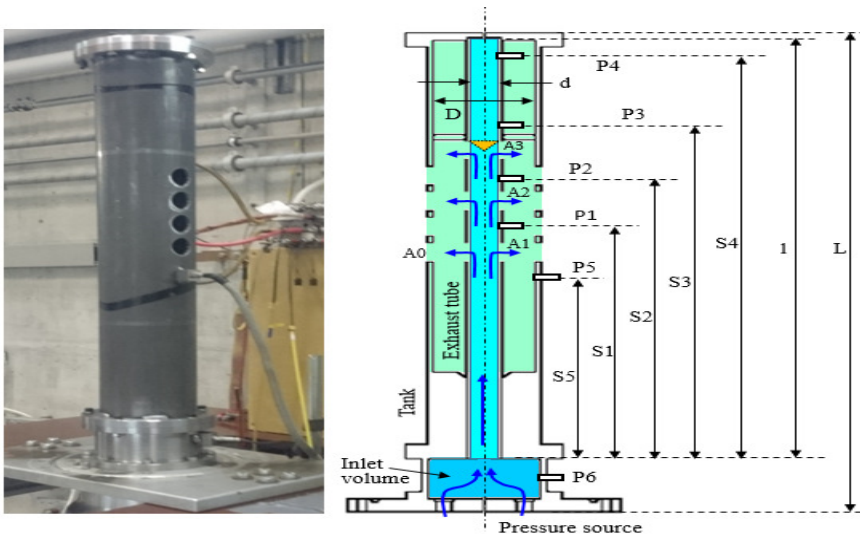


**Figure 2.** Experimental set-up of exhaust tube study.

Figure 2 shows the experimental set-up for the exhaust tube study. The tank has the length of  $L$  and inner diameter of  $D$ . There are 2 rows with 4 circular holes in each row in the middle of the tank and the two rows are placed in an angle of  $180^\circ$ . On the bottom side, the tank is connected through several holes to a  $\text{CO}_2$  vessel as the pressure source. The exhaust tube is located in the tank with inner diameter  $d$ , and length  $l$ . It has 3 columns of holes and each row has two holes placed in an angle of  $180^\circ$ . The exhaust hole columns with area of  $A_1$ ,  $A_2$  and  $A_3$  are distributed along the exhaust tube;

pressure sensors P1 – P5 are put along the tube inner surface with different distance from bottom S1-S5. Pressure sensor P6 is put in the middle of inlet volume. In Test 1, the exhaust tube is blocked with a conical body at end of hole A1 as shown in Figure 2 with orange colour. In all other tests, the exhaust tube is not blocked with the conical body, hence, there is a dead volume above the hole column A3.

Table 1 shows the position and area normalized against the exhaust tube diameter and its area for each test. In Test 1, since the dead volume above the hole column A3 is blocked, no pressure measurement at position S3 and S4 is available, while Test 2 to 4 have the pressure measurement in the dead volume. Test 1 and Test 2 have the same uniform hole column area, while Test 3 has small (S), medium (M) and large (L) hole column distribution (SML) and Test 4 has LMS hole column distribution along the flow direction.

## 2.2 Testing procedure

In every test, the whole test device is placed under ambient air, i.e., is filled with air with atmosphere pressure initially. At the start of the test, the CO<sub>2</sub> pressure vessel valve is opened, so that the CO<sub>2</sub> gas flows through several connecting holes into the initial volume and further into the exhaust tube. Finally the gas flows into the tank and through the tank holes to the atmosphere. During the test, the pressure at different positions is measured and saved with a transient recorder.

**Table 1.** Test number and the corresponding geometry parameters normalized against exhaust tube area (A) or exhaust tube diameter.

Test number	A1/A	A2/A	A3/A	A0/A	S1/d	S2/d	S3/d	S4/d	S5/d
1	0.58	0.58	0.58	0.86	21.8	26.7	none	none	16.6
2	0.58	0.58	0.58	0.86	21.8	26.7	31.6	38.2	16.6
3	0.14	0.72	0.86	0.86	21.8	26.7	31.6	38.2	16.6
4	0.86	0.72	0.14	0.86	21.8	26.7	31.6	38.2	16.6

## 3 CFD simulation

### 3.1 Mathematical model

The main parameters of CFD simulation, namely pressure, density, temperature and gas velocity, are solved with the Navier-Stokes equations for the conservation of mass, momentum and energy. These equations are discretized and solved iteratively using a commercial finite volume solver. The application and implementation of arc model are described in detail [1-5] and are not discussed in this work. For the sake of completeness, a brief model description and numerical details are provided:

Energy source terms are added to represent the effect of the arc on the flow: ohmic heating is added based on the solution of the electric field distribution inside the arc and the radiative transfer is computed based on discrete ordinate method (DOM) approximating the radiation transfer equation on 12 ordinate directions [5]. Electric field is computed statically using a simple Laplace equation for the electric potential. The mass source term is added to represent the effect of PTFE nozzle material ablation and the erosion of the arcing contacts as in [6] and [7]. In order to take turbulence effects into account the realizable k-ε model [6] is used. A numerical scheme is used for the pressure – velocity coupling due to its suitability for transient calculations. Thermodynamic and transport properties of the mixture in pressure and temperature range are calculated assuming local thermal equilibrium conditions [8] and tabulated in the form of look-up tables, retrieved by the solver during calculation.

### 3.2 Numerical discretization

Thermodynamic and transport properties of the mixture in the pressure and temperature range are calculated assuming local thermal equilibrium conditions, tabulated in the form of look-up tables and retrieved by the solver during calculation. The model equations are discretized and solved on a hybrid block-structured and unstructured mesh. The numbers of cells in the discretization are in the range of 150-200 K for a 2D model. More details about the model and numerical methods are given in [5].

To limit the calculation time, two-dimensional (2D) simulation is selected, instead of three-dimensional (3D) simulation and the breaker model is simplified to a smaller part to focus on the main problem of the study.

## 4 Result and discussion

### 4.1 Validation of CFD method

Figure 3 shows the CFD set-up for the validation calculation. Because of the complex flow conditions in the apparatus connecting the test device and the CO<sub>2</sub> pressure vessel with valve and pipe, the measured pressure in the CO<sub>2</sub> vessel cannot be used as the inlet pressure boundary condition, hence, the measured pressure in the inlet volume is used as the total inlet pressure with CO<sub>2</sub> species. The atmosphere pressure 1 bar is taken as the outlet pressure boundary condition. The initial condition is set with 1 bar filled with air as in the experiment.

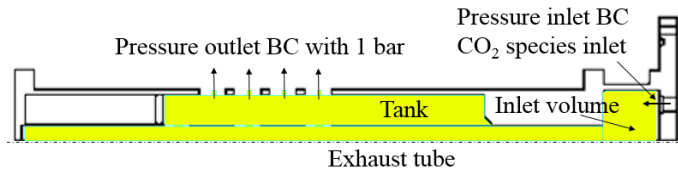


**Figure 3.** CFD simulation set-up and meshing with the yellow region for the validation.

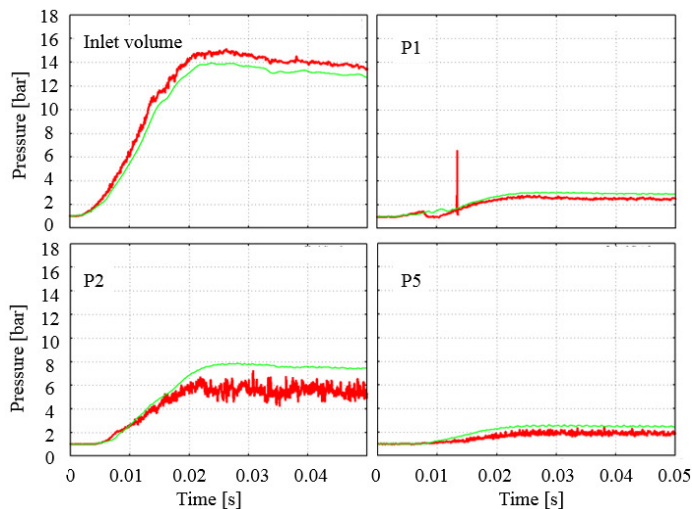
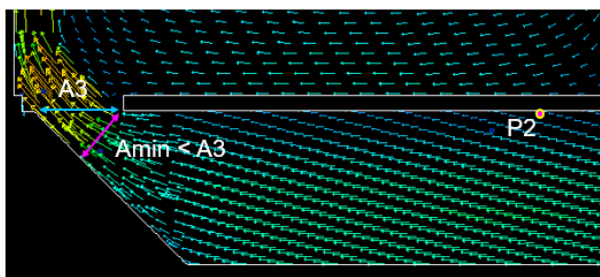


**Figure 4.** Comparison of simulated pressure distribution to the measurement: Test 1 with red lines, green lines of simulation.

As shown in Figure 4, for Test 1 with uniform hole column area and blocked dead volume, the simulated pressure is compared against the measured pressure in the inlet volume, at position P1, P2 and P5. The spike in the measured pressure signal of P1 is a disturbance or noise in the pressure measuring system and have normally no influence on the measurement in general. The agreement

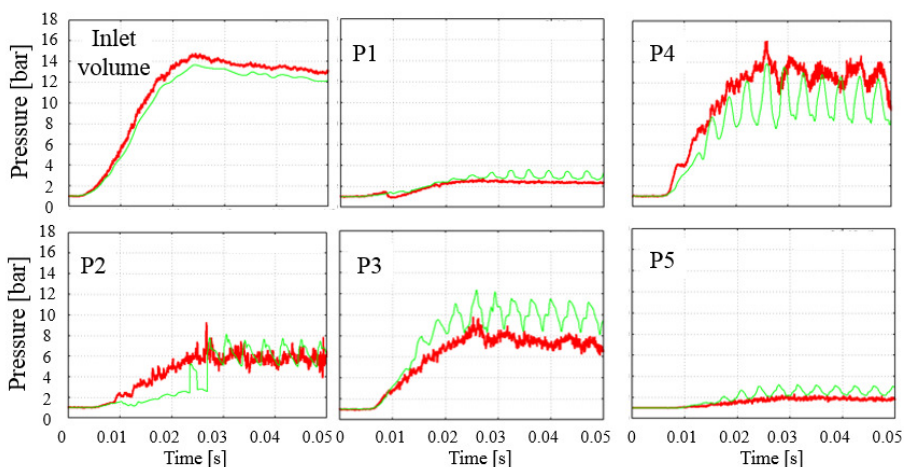
between simulation and experiment is reasonably good. Since the result differ by less than 5%, the use of the pressure in the inlet volume as the inlet pressure boundary condition is justified.

The agreement between measurement and simulation at P1 is better than at P2, suggesting that the 3D geometrical configuration at hole column A3 has much less influence on the pressure P1. The bigger deviation at P2 comes from the 2-dimensional modelling of the flow area between the hole column A3 and the conical body as shown in Figure 5. If the resulting minimum area is too small, the local flow velocity will be too low, and consequently the local pressure at P2, too high. Therefore, a more accurate result can be only achieved with 3D simulation.



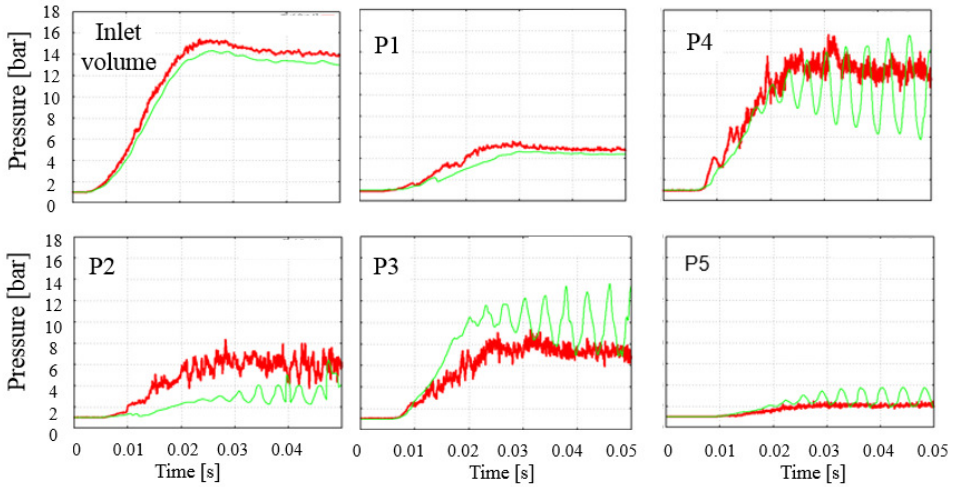
**Figure 5.** 2-dimensional modelling of 3D geometrical configuration of hole A3 and the conical body.

Figure 6 shows the comparison of measurement and simulation for Test 2 with uniform hole column area and dead volume. The agreement in general is satisfactory especially the measurement of P3 that confirms the pressure oscillation in the dead volume above the hole column A3. The simulated pressure at P2 shows a transient effect of 2-dimensional modelling in the first 30 ms, after which the pressure recovers to the measured value. Besides this, the 2-dimensional modelling also shows an overall pronounced pressure oscillation which is induced through the Helmholtz oscillation in the dead volume. This can be seen clearly by comparing the simulation results in Figure 5 of Test1 and Figure 6 of Test 2. In practice the oscillation is damped for P1 and P5 as is suggested by 3D simulation.



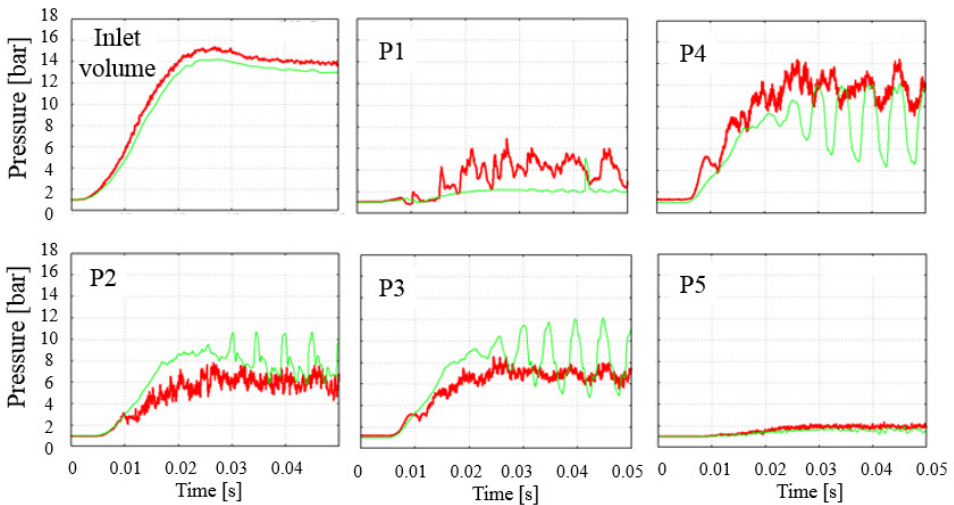
**Figure 6.** Comparison of simulated pressure distribution to the measurement: Test 2 results with red lines, green lines of simulation.

Figure 7 shows the results of Test 3 with SML hole column distribution. Due to a transient effect, the simulated pressure at P2 reaches the measured value after 40 ms. P1 indicates a good agreement without pronounced pressure oscillation, while the simulation for P3, P4, and P5 show a pronounced pressure oscillation.



**Figure 7.** Comparison of simulated pressure distribution to the measurement: Test 3 results with red lines, green lines of simulation.

Figure 8 shows the results for Test 4 with LMS circular hole distribution. Here the measured pressure at P1 shows a pronounced pressure oscillation, which is absent in the simulation. The pressure measurement of P2, P3 and P4 all show a moderate pressure oscillation, but the simulation gives a more pronounced pressure oscillation. This behaviour can be explained again with 2-dimensional modelling for the 3D geometrical holes. The highly asymmetrical hole configuration exhibits different pressure oscillation behaviour. This should be checked further with 3D simulation.



**Figure 8.** Comparison of simulated pressure distribution to the measurement: Test 4 results with red lines, green lines of simulation.

The validation confirms that the 2D simulation reflects the general behaviour of exhaust tube, although with some deviation. This confirmation significance for further investigations, since the exhaust tube simulation with arcing zone represents the exhaust tube in a real breaker. 3D arc simulation requires much longer calculation time and often suffers problems with numerical instability, therefore, 2D arc simulation is generally preferred.

### 4.2 Arc simulation of exhaust tube

Figure 9 shows a typical CFD set-up for the arc simulation of exhaust tube. The exhaust tube is connected to the arcing zone which consists of arcing contacts, heating volume, and nozzles. The temperature generated by the arc affects the flow field in the breaker, they are coupled and interact with each other and are considered in the governing equation system of the mathematical model of the CFD code. To simplify the simulation, arcing contacts have a constant opening gap with no movement. The model is further simplified by setting the outlet pressure boundary condition of the filling pressure, to between 6 and 10 bar depending on the switching gas.

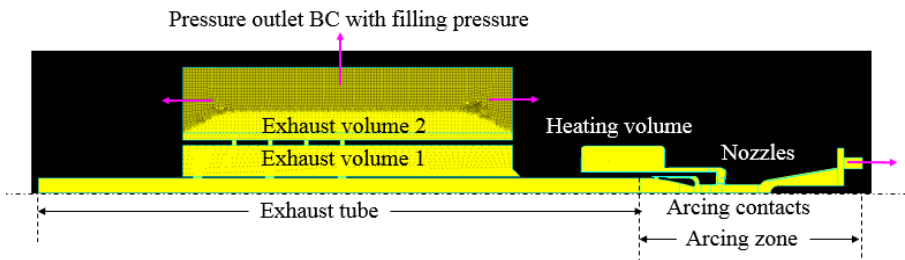


**Figure 9.** CFD set-up for the arc simulation of exhaust tub.

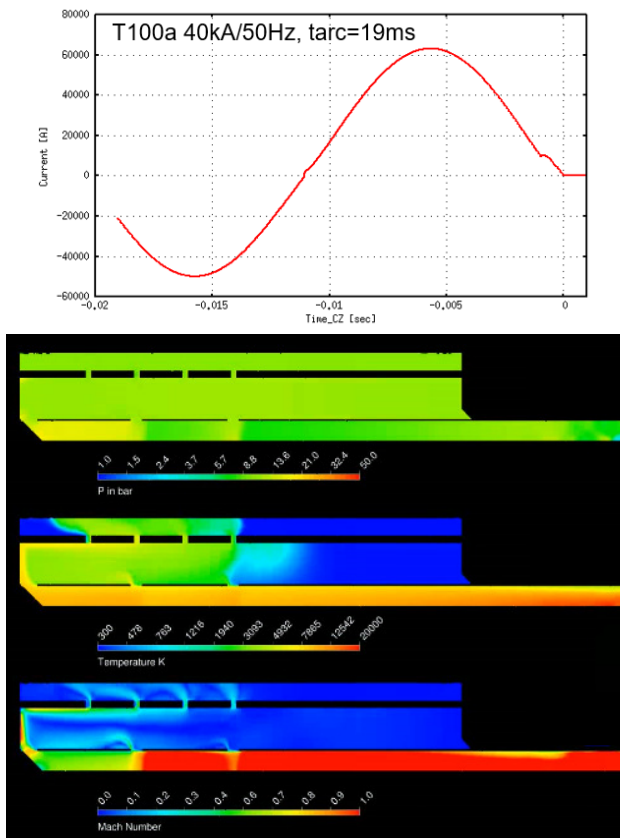


**Figure 10.** Typical current and flow pattern of arc simulation for an exhaust tube with CO<sub>2</sub>.

Figure 10 shows a typical flow pattern from the arc simulation of exhaust tube at current peak of T100a long arcing time case. It can be seen that the Mach number and pressure can change locally with the hole position. This affects the mass flow through holes.

Two parameters can be used to describe the hot gas evacuation in the exhaust tube:

- Total mass through holes: It is the sum of the integral of the mass flow through all exhaust holes. Figure 11 shows the total mass through holes of different exhaust tube. It can be seen that the lowest mass through holes is the variant with LMS configuration. The highest mass through holes can be obtained with the variant consisting stepwise expansion tube.

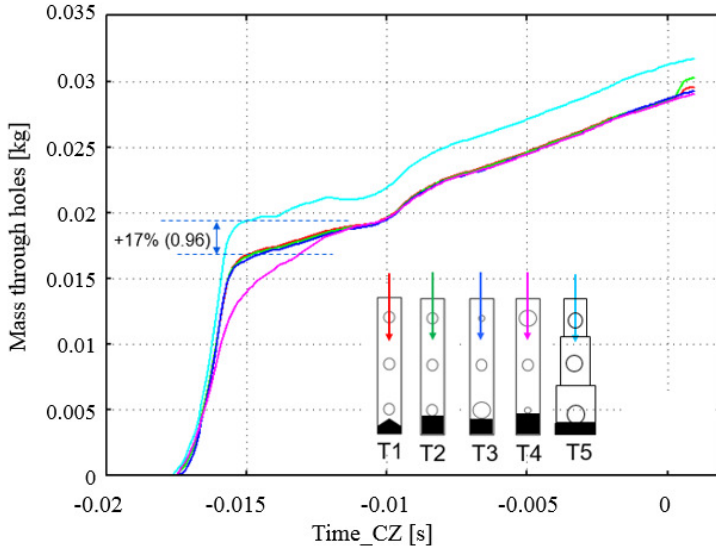


**Figure 11.** Total mass through holes of different exhaust tube, T100a, 19ms arcing time.

- Exhaust tube efficiency: It is defined as the ratio of the inlet mass flow and the outlet mass flow  $\eta = \dot{m}_{out} / \dot{m}_{in}$ . The exhaust tube efficiency of different variants is compared in Figure 12. It can be seen that again the lowest exhaust tube efficiency is the variant with LMS configuration. The highest efficiency can be obtained with the variant consisting stepwise expansion tube

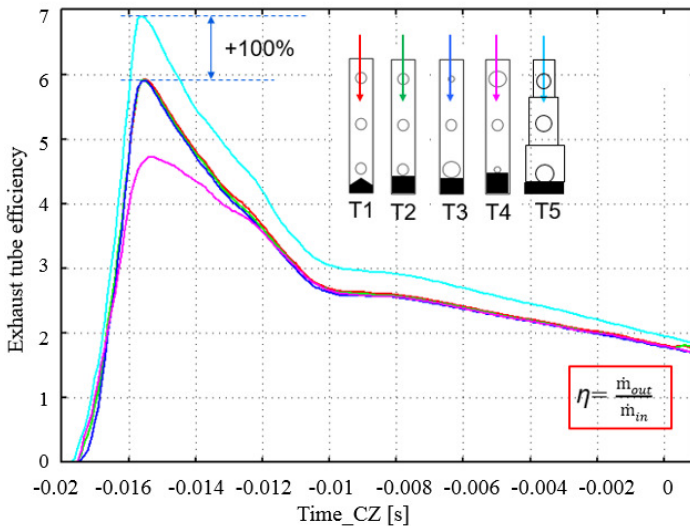


**Figure 12.** Exhaust tube efficiency of different exhaust tube, T100a, 19ms arcing time.

With these two parameters, exhaust tube design can be done essentially to fulfil the requirement for the current interruption.

## 5 Conclusion

Based on the comparison against the experimental study, the CFD simulation is validated and its accuracy and limitation in the 2D modelling of the 3-dimensional configuration is established.

The total mass through holes and the exhaust tube efficiency can be used to quantify the exhaust tube performance according to the requirement of current interruption. Expressed in terms of these two performance metric parameters, the exhaust tube with expanding sections seems to be the variant that delivers the best exhaust tube performance.

## References

1. C.M. Claessens and G. Speckhofer, *CFD-Simulation of electrical arcs in circuit-breakers, Proceedings of ASME/JSME Conference*, San Diego (1998)
2. X. Ye, A. Dahlquist, J. Abrahamsson and C. Franck, *CFD simulation of heat transfer and gas mixing in exhaust parts of high-voltage circuit breaker, Proceedings of IEEE International Symposium on Electrical Insulation*, Vancouver, Canada, June 9-12 (2008)
3. H. Nordborg and A. Iordanidis, *Journal of Physics D: Applied Physics*, **41**(13), 135205 (2008)
4. M. Dhotre, X. Ye, S. Kotilainen, M. Schwinne and R. Bini, *CFD simulation for self-blast high voltage circuit breaker: Mixing and Heat transfer, Proceedings of the Electrical Insulation Conference*, Annapolis, Maryland, USA, June 5-8 (2011)
5. A. A. Iordanidis and C. M. Franck, *Journal of Physics D: Applied Physics*, **41**(13), 135206 (2008)
6. L. Niemeyer, *IEEE Transactions on Power Apparatus and Systems*, **PAS-97**(3), 950-958 (1978)
7. C.B. Ruchti and L. Niemeyer, *IEEE Trans. Plasma Sci.*, **PS-14**(4), 423-434 (1986)
8. X. Ye, M.T. Dhotre, J.D. Mantilla and S. Kotilainen, *CFD Analysis of the Thermal Interruption Process of Gases with Low Environmental Impact in High Voltage Circuit Breakers, Proceedings of the Electrical Insulation Conference*, Seattle, WA, USA June 7-10 (2014)